



HAL
open science

The conduit equation : hyperbolic approximation and generalized Riemann problem

Sergey Gavriluk, Boniface Nkonga, Keh-Ming Shyue

► **To cite this version:**

Sergey Gavriluk, Boniface Nkonga, Keh-Ming Shyue. The conduit equation : hyperbolic approximation and generalized Riemann problem. 2024. hal-04377682

HAL Id: hal-04377682

<https://hal.science/hal-04377682>

Preprint submitted on 7 Jan 2024

HAL is a multi-disciplinary open access archive for the deposit and dissemination of scientific research documents, whether they are published or not. The documents may come from teaching and research institutions in France or abroad, or from public or private research centers.

L'archive ouverte pluridisciplinaire **HAL**, est destinée au dépôt et à la diffusion de documents scientifiques de niveau recherche, publiés ou non, émanant des établissements d'enseignement et de recherche français ou étrangers, des laboratoires publics ou privés.

The conduit equation : hyperbolic approximation and generalized Riemann problem

Sergey Gavriluk*, Boniface Nkonga †, Keh-Ming Shyue ‡

January 4, 2024

Abstract

The conduit equation is a dispersive non-integrable scalar equation modeling the flow of a low-viscous buoyant fluid embedded in a highly viscous fluid matrix. This equation can be written in a special form reminiscent of the famous Godunov form proposed in 1961 for the Euler equations of compressible fluids. We propose a hyperbolic approximation of the conduit equation by retaining the Godunov-type structure. The comparison of solutions to the conduit equation and those to the approximate hyperbolic system is performed : the wave fission of a large initial perturbation of a rectangular or of gaussian form. The results are in good agreement. New generalized solutions to the conduit equation are discovered composed of a finite set of waves of the same period and linked with a constant solution by generalized Rankine-Hugoniot relations. Such multi-hump structures interact which each other almost as solitary waves : they collide, merge and reconstruct after the interaction. This partly indicates the stability of such multi-hump solutions under small perturbations. Both the exact and approximate hyperbolic system describe such an interaction with good accuracy.

Keywords : **Mathematics Subject Classification numbers:** 35L40, 35Q35, 35Q74.

1 Introduction

Consider the *conduit equation* :

$$u_t + (u^2 + u_x u_t - u u_{tx})_x = 0, \quad (1)$$

*Corresponding author, Aix Marseille University, CNRS, IUSTI, UMR 7343, Marseille, France, sergey.gavrilyuk@univ-amu.fr

†Université de Nice Sophia-Antipolis, CNRS UMR 7351, Laboratoire J.A.Dieudonné, Parc Valrose, 06108 NICE Cedex 2 France, Boniface.Nkonga@unice.fr

‡Institute of Mathematical Sciences, National Taiwan University, Taipei 106, Taiwan, shyue@ntu.edu.tw

involving one dependent variable $u(t, x)$ and two independent variables t (time) and x (space coordinate). Physically, the equation (1) represents the mass conservation law written in dimensionless variables for the magnitude $u(t, x)$ of the non-dimensional circular cross-section of a low-viscosity buoyant fluid embedded in a highly viscous fluid at rest (cf. [29, 22, 23, 24, 27, 26, 25]). Hence, only positive solutions $u(t, x)$ are physically admissible. Another conservative form which, *a priori*, has no physical meaning can be found for the conduit equation :

$$\left(\frac{1}{u} + \frac{u_{xx}}{u} \right)_t - (2 \ln(u))_x = 0. \quad (2)$$

Its mathematical importance will be shown later. The dispersion relation for the conduit equation linearized on the solution $u = u_0 = \text{const} > 0$ can be written as

$$c_p = \frac{2u_0}{1 + u_0 k^2}, \quad (3)$$

where k is the wave number, and c_p is the corresponding phase velocity. It has the same dispersive properties as the Benjamin-Bona-Mahony (BBM) equation [1]. The derivation of the modulation equations to the conduit equation and their stability study for small amplitude waves has been performed in [26, 16].

In [8, 6, 4, 10, 2, 32], a general method of hyperbolic regularization of dispersive equations that are the Euler-Lagrange equations for a “master” Lagrangian has been proposed: the original high order derivative dispersive equations were approximated by a first order hyperbolic system of the Euler-Lagrange equations for a one or two parameter family of “extended” Lagrangians. The “master” Lagrangian is obtained from the “extended” Lagrangian in some limit. Thus, the variational structure of the governing equations was conserved. In a particular case of long gravity surface waves described by the Serre-Green-Naghdi equations, the method of “extended Lagrangian” was mathematically justified in [7]. The advantage of such an approach is obvious: one can use for dispersive equations the full range of finite volume methods developed for hyperbolic equations. Furthermore, some non-linear dispersive equations admit shock-type solutions: the dispersion cannot always prevent the formation of such singularities [11, 9]. Thus, the study of such singularities can be done much more easily when the hyperbolic approximation is used.

Despite a large number of works on the conduit equation, unlike the almost similar BBM equation (at least in the linear limit), neither other linearly independent conservation laws for this equation, nor the existence of a Lagrangian allowing this equation to be considered as the Euler-Lagrange equation, are known [16]. Having in mind to approximate the conduit equation by a system of hyperbolic equations, we then ask the following question: what is the mathematical structure (different from a classical variational structure) of the conduit equation, and should it be retained when the equation is approximated by a system of hyperbolic equations?

In this paper, we will exhibit such a structure and will formulate an approximating hyperbolic system of equations conserving this structure. The compar-

ison of numerical solutions to the exact conduit equation and to its “structure conserving” hyperbolic approximation show a very good convergence results.

2 Mathematical structure of the conduit equation

In 1961 [13] S. K. Godunov proposed the following abstract form of a system of conservation laws for the vector variable $\mathbf{v} = (v_1, \dots, v_n)^T$:

$$\left(\frac{\partial L^0(\mathbf{v})}{\partial \mathbf{v}} \right)_t + \sum_{i=1}^m \left(\frac{\partial L^i(\mathbf{v})}{\partial \mathbf{v}} \right)_{x_i} = 0, \quad (4)$$

with given functions (potentials) $L^i(\mathbf{v})$, $i = 0, \dots, m$. This system admits an additional conservation law

$$\left(\frac{\partial L^0(\mathbf{v})}{\partial \mathbf{v}} \cdot \mathbf{v} - L^0(\mathbf{v}) \right)_t + \sum_{i=1}^m \left(\frac{\partial L^i}{\partial \mathbf{v}} \cdot \mathbf{v} - L^i \right)_{x_i} = 0. \quad (5)$$

If the Hessian matrix of L^0 is positive definite, the equations can be written in the symmetric form of Friedrichs. Denoting the variable t by x_0 , we can rewrite the system (4) and its consequence (5) in a compact form :

$$\frac{\partial}{\partial x^\beta} \left(\frac{\partial L^\beta}{\partial v^\alpha} \right) = 0, \quad \frac{\partial E^\beta}{\partial x^\beta} = 0, \quad E^\beta = v^\alpha \frac{\partial L^\beta}{\partial v^\alpha} - L^\beta, \quad (6)$$

with $\beta = 0, \dots, m$, $\alpha = 1, \dots, n$. Here the summation is taken over repeated indexes. A number of *reversible* models of continuum mechanics can be written in Godunov’s form (6) [14].

A generalization of such a class of models with multiple examples coming from the reversible continuum mechanics was proposed in [12], with potentials L^β depending not only on unknowns but also on their first derivatives. More precisely, let us denote $v_{,\gamma}^\alpha = \frac{\partial v^\alpha}{\partial x^\gamma}$. Consider functions $L^\beta(v^\alpha, v_{,\gamma}^\alpha)$ (we will use the same notations as for the old potentials L^β depending only on v^β) and a conservative system in the form

$$\frac{\partial}{\partial x^\beta} \left(\frac{\delta L^\beta}{\delta v^\alpha} \right) = 0. \quad (7)$$

Here we used usual notation for the variational derivatives :

$$\frac{\delta L^\beta}{\delta v^\alpha} = \frac{\partial L^\beta}{\partial v^\alpha} - \frac{\partial}{\partial x^\gamma} \left(\frac{\partial L^\beta}{\partial v_{,\gamma}^\alpha} \right).$$

Equations (7) also admit an additional conservation law

$$\frac{\partial E^\beta}{\partial x^\beta} = 0, \quad E^\beta = v^\alpha \frac{\delta L^\beta}{\delta v^\alpha} - L^\beta + v_{,\gamma}^\alpha \frac{\partial L^\beta}{\partial v_{,\gamma}^\alpha}. \quad (8)$$

Let us rewrite the conduit equation in the form (7). For this, we will use the conservative form (2) with $x^0 = t$ and $x^1 = x$. Let us consider the change of variables

$$u = \sqrt{1 + 2v} \quad (9)$$

and potentials $L(v, v_x)$ and $M(v)$ (instead of generic potentials L^0 and L^1) defined as :

$$L(v, v_x) = \sqrt{1 + 2v} - \frac{v_x^2}{2(1 + 2v)}, \quad M(v) = -\frac{1}{2}(1 + 2v)(\ln(1 + 2v) - 1). \quad (10)$$

Then, one obtains :

$$\frac{\delta L}{\delta v} = \frac{1}{\sqrt{1 + 2v}} + \frac{v_{xx}}{1 + 2v} - \frac{v_x^2}{(1 + 2v)^2} = \frac{1 + u_{xx}}{u} = \frac{1}{u} + \frac{u_{xx}}{u}. \quad (11)$$

$$\frac{\partial M(v)}{\partial v} = -\ln(1 + 2v) = -2 \ln(u). \quad (12)$$

Hence, the equation (2) is written of the form (7):

$$\left(\frac{\delta L(v, v_x)}{\delta v} \right)_t + \left(\frac{\partial M(v)}{\partial v} \right)_x = 0, \quad (13)$$

The equation (13) admits an additional conservation law :

$$\left(v \frac{\delta L}{\delta v} - L \right)_t + \left(v_t L_{v_x} + v \frac{\partial M}{\partial v} - M \right)_x = 0. \quad (14)$$

Unfortunately, it is not a new conservation law, but just a linear combination of (1) and (2). The equations (13) also admit a ‘‘symmetric’’ form. Indeed, consider the partial Legendre transform of L :

$$L^*(v, w) = wv_x - L(v, v_x), \quad \text{where } w = L_{v_x}. \quad (15)$$

It implies, by using the implicit function theorem,

$$L_v^* = -L_v, \quad L_w^* = v_x. \quad (16)$$

It allows thus to rewrite (13) as

$$(L_v^*)_t - (M'(v))_x + w_{tx} = 0, \quad (L_w^*)_t - v_{tx} = 0. \quad (17)$$

Or

$$\begin{pmatrix} L_{vv}^* & L_{vw}^* \\ L_{vw}^* & L_{ww}^* \end{pmatrix} \begin{pmatrix} v \\ w \end{pmatrix}_t - \begin{pmatrix} M''(v) & 0 \\ 0 & 0 \end{pmatrix} \begin{pmatrix} v \\ w \end{pmatrix}_x + \begin{pmatrix} 0 & 1 \\ -1 & 0 \end{pmatrix} \begin{pmatrix} v \\ w \end{pmatrix}_{tx} = 0. \quad (18)$$

The form (18) contains also a skew symmetric matrice multiplied by a vector of mixed derivatives.

3 Extended hyperbolic system

The idea of the hyperbolic approximation of the equation (1) is to replace it by an “extended” parametric family of reversible hyperbolic systems having also the Godunov-type form (7). The word “extended” means that the governing equations contain an extra unknown $z(t, x)$ which is asymptotically close to the unknown $u(t, x)$ when parameters of the model go to infinity. Such a “penalization” method was already used in [8, 6, 4, 10, 2, 3] for mathematical models admitting a variational formulation. The “extended” system of equations was obtained as the Euler-Lagrange equations for an “extended” Lagrangian. Equation (13) does not correspond to any Euler-Lagrange equation. Indeed, it involves two potentials, L and M , while the Euler-Lagrange equations are written in terms of a single potential (Lagrange function). Doing so, we expect a better approximation of the conduit equation by the corresponding hyperbolic system of equations.

Consider a two-parameter family of potentials

$$\mathcal{L}(v, z, z_x, z_t) = \sqrt{1 + 2v} + \frac{z_t^2}{2c^2} - \frac{z_x^2}{2} - \frac{\lambda}{2} (z - \sqrt{1 + 2v})^2, \quad (19)$$

where λ and c are large parameters. Let us replace the equation (13) by a system of equations for two unknowns v and z :

$$\left(\frac{\partial \mathcal{L}}{\partial v} \right)_t + \left(\frac{\partial M}{\partial v} \right)_x = 0, \quad \frac{\delta \mathcal{L}}{\delta z} = 0, \quad (20)$$

with

$$\frac{\delta \mathcal{L}}{\delta z} = \mathcal{L}_z - (\mathcal{L}_{z_t})_t - (\mathcal{L}_{z_x})_x.$$

It admits the conservation law :

$$(z_t \mathcal{L}_{z_t} + v \mathcal{L}_v - \mathcal{L})_t + (z_t \mathcal{L}_{z_x} + v M_v - M)_x = 0, \quad (21)$$

i.e., it conserves the structure of the system (13). Indeed,

$$(z_t \mathcal{L}_{z_t} + v \mathcal{L}_v - \mathcal{L})_t + (z_t \mathcal{L}_{z_x} + v M_v - M)_x = -z_t \frac{\delta \mathcal{L}}{\delta z} = 0.$$

Let us also remark that if one introduces a function $\varphi(t, x)$ instead of variable $z(t, x) : z = \varphi_t$, the equation for z can be written in equivalent form as

$$\left(\frac{\delta \mathcal{L}}{\delta z} \right)_t = \frac{\delta \mathcal{L}}{\delta \varphi} = 0.$$

Now we will write the equations (20) in explicit form by using the expressions

for derivatives :

$$\frac{\partial \mathcal{L}}{\partial v} = \frac{1}{\sqrt{1+2v}} + \lambda \frac{z - \sqrt{1+2v}}{\sqrt{1+2v}}, \quad (22a)$$

$$\frac{\partial \mathcal{L}}{\partial z} = -\lambda (z - \sqrt{1+2v}), \quad (22b)$$

$$\frac{\partial \mathcal{L}}{\partial z_x} = -z_x, \quad (22c)$$

$$\frac{\partial \mathcal{L}}{\partial z_t} = \frac{z_t}{c^2}. \quad (22d)$$

The first equation of (20) becomes :

$$\left(\frac{1}{\sqrt{1+2v}} + \lambda \frac{z - \sqrt{1+2v}}{\sqrt{1+2v}} \right)_t - \frac{2}{1+2v} v_x = 0. \quad (23)$$

The second equation of (20) becomes :

$$-\frac{1}{c^2} z_{tt} + z_{xx} = \lambda (z - \sqrt{1+2v}). \quad (24)$$

Finally, we return back to u -variable ($u = \sqrt{1+2v}$):

$$\left(\frac{1}{u} + \lambda \frac{z-u}{u} \right)_t - \frac{2u_x}{u} = 0, \quad -\frac{1}{c^2} z_{tt} + z_{xx} = \lambda (z-u). \quad (25)$$

Similar to the conduit equation, this system is reversible in the sense that it is invariant under the change of independent variables $t \rightarrow -t$, $x \rightarrow -x$. Its first order quasi-linear formulation can then be written as :

$$\left(\frac{1}{u} + \lambda \frac{z-u}{u} \right)_t - \frac{2u_x}{u} = 0, \quad (26a)$$

$$-\frac{1}{c} z_t + z_x = p, \quad (26b)$$

$$\frac{1}{c} p_t + p_x = \lambda (z-u). \quad (26c)$$

The eigenvalues are $\pm c$ and $2u/(1+\lambda z)$. Hence, for large enough c and λ , the equations are hyperbolic. The initial conditions for (26) are :

$$u(0, x) = u_0(x), \quad z(0, x) = u_0(x), \quad p(0, x) = \frac{du_0(x)}{dx}. \quad (27)$$

These are the conditions we used for the benchmark tests in Section 7. In the following, we will take $\lambda = c^2$. The system (25) admits the conservation law (21) which is equivalent to the following one :

$$\left(\frac{z_t^2}{c^2} + z_x^2 + \lambda z^2 - u(1+\lambda z) \right)_t - (u^2 + 2z_t z_x)_x = 0. \quad (28)$$

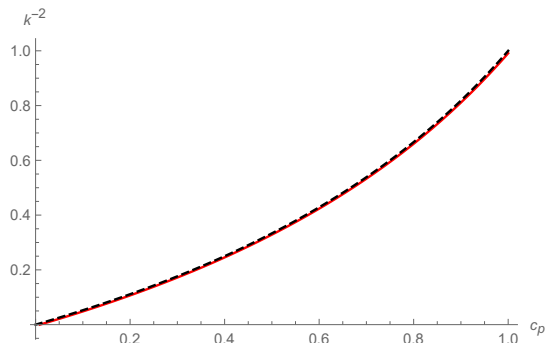


Figure 1: Comparison of the exact dispersion relation for $u_0 = 1$ (black dashed curve) and approximate one (red curve for $c = 15$, $\lambda = c^2 = 225$) is shown.

4 Dispersion relation

The dispersion relation for the hyperbolic system (26) linearized on the solution $u = u_0$, $z = u_0$, $p = 0$ is :

$$\frac{1}{k^2} = \frac{1 + \lambda u_0 (c_p^2/c^2 - 1)(c_p - 2u_0/(1 + \lambda u_0))}{\lambda (c_p - 2u_0)}. \quad (29)$$

For any wave number k the real root c_p approximating the exact dispersion relation (3) satisfies the inequality

$$\frac{2u_0}{1 + \lambda u_0} < c_p < 2u_0. \quad (30)$$

For large λ and c^2 the approximate dispersion relation can be written as :

$$\frac{1}{k^2} = \frac{c_p u_0}{2u_0 - c_p} + \mathcal{O}\left(\frac{1}{\lambda} + \frac{1}{c^2}\right). \quad (31)$$

Figure (4) shows the “quality” of the approximate dispersion relation (29). The asymptotic formula (31) suggests a natural choice of $\lambda = c^2$ to pass to one parameter family of penalty functions $\mathcal{L}(v, z, z_t, z_x)$ defined by (19).

5 Periodic solutions

Periodic and solitary wave solutions to the conduit equation can be found, for example, in [29]. Here a quick overview of the solutions is given. Looking for traveling solutions to (2) depending only on $\xi = x - Dt$, $D = \text{const} > 0$ is the wave velocity, one obtains the ODE :

$$Du'' = (C - 1)u - 2u \ln(u) - D, \quad C = \text{const}, \quad (32)$$

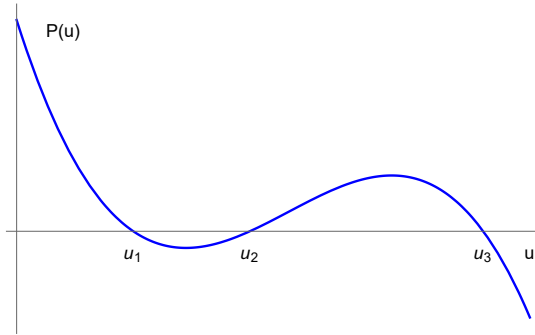


Figure 2: A typical behavior of the function $P(u)$ is shown. In a domain of parameters $C, D > 0, Q < 0$ it has three roots $0 < u_1 < u_2 < u_3$. The periodic solution oscillates between u_2 and u_3 .

admitting the first integral

$$Du'^2 = P(u) = Cu^2 - 2u^2 \ln(u) - 2Du - Q, \quad Q = \text{const.} \quad (33)$$

Here “prime” means the derivative with respect to ξ . Since $u \ln(u)$ is convex for $u > 0$, the function $P(u)$ has maximum two critical points for $u > 0$, and hence maximum three roots. In the last case we denote them u_i , $P(u_i) = 0$, $i = 1, 2, 3$, $0 < u_1 < u_2 < u_3$. A typical behavior of $P(u)$ is shown in Figure 5. One can construct periodic solution oscillating between u_2 (minimum of the wave amplitude) and u_3 (maximum of the wave amplitude). The case $u_1 = u_2$ gives the solitary wave solutions. The wave velocity D , and the constants C and Q are thus calculated from the linear system :

$$Cu_i^2 - 2u_i^2 \ln(u_i) - 2Du_i - Q = 0, \quad i = 1, 2, 3. \quad (34)$$

Its solution is unique if $u_1 \neq u_2 \neq u_3$. The wave length L and averaged over the wave length the periodic solution \bar{u} are given by the following expressions coming directly from (33):

$$L = 2\sqrt{D} \int_{u_2}^{u_3} \frac{du}{\sqrt{P(u)}}, \quad \bar{u} = \frac{\int_{u_2}^{u_3} \frac{udu}{\sqrt{P(u)}}}{\int_{u_2}^{u_3} \frac{du}{\sqrt{P(u)}}}. \quad (35)$$

To study traveling wave solutions to (26), we will use the conservative form of equations :

$$\begin{aligned} \left(\frac{1}{u} + \lambda \frac{z-u}{u} \right)_t - (\ln(u^2))_x &= 0, \\ \left(\frac{z_t^2}{c^2} + z_x^2 + \lambda z^2 - u(1 + \lambda z) \right)_t - (u^2 + 2z_t z_x)_x &= 0. \end{aligned}$$

Using again the sign “prime” for the derivative with respect to the traveling wave coordinate $\xi = x - Dt$, one gets the following ODE system

$$-D \left(\frac{1}{u} + \lambda \frac{z-u}{u} \right) - \ln(u^2) = c_1, \quad (36a)$$

$$D \left(1 - \frac{D^2}{c^2} \right) z'^2 = D(\lambda z^2 - u(1 + \lambda z)) + u^2 + c_2, \quad (36b)$$

where c_i , $i = 1, 2$ are constants. It can be reduced to only one equation for u . Indeed, one has

$$z = u - \frac{u}{D\lambda} \left(c_1 + \ln(u^2) + \frac{D}{u} \right), \quad (36c)$$

that yields

$$\frac{dz}{du} = 1 - \frac{1}{D\lambda} (c_1 + 2 + 2 \ln(u)). \quad (36d)$$

Then the equation (36b) becomes

$$D \left(1 - \frac{D^2}{c^2} \right) \left(1 - \frac{1}{D\lambda} (c_1 + 2 + 2 \ln(u)) \right)^2 (u')^2 = \frac{u^2}{D\lambda} \left(D\lambda - c_1 - 2 \ln(u) - \frac{D}{u} \right)^2 - D\lambda u^2 + c_1 u^2 + u^2 + 2u^2 \ln(u) + c_2$$

Finally, a compact form of this equation is :

$$(u')^2 = \frac{F(u)}{G(u)}, \quad (37a)$$

where

$$F(u) = \frac{u^2}{D\lambda} \left(D\lambda - c_1 - 2 \ln(u) - \frac{D}{u} \right)^2 + u^2 (1 + c_1 - D\lambda + 2 \ln(u)) + c_2, \quad (37b)$$

$$G(u) = D \left(1 - \frac{D^2}{c^2} \right) \left(1 - \frac{1}{D\lambda} (c_1 + 2 + 2 \ln(u)) \right)^2. \quad (37c)$$

To find the solution of (37) numerically using an ODE solver, we need to determine the parameters c_1 , c_2 , and D first. Given three constant states u_1 , u_2 , and u_3 , $0 < u_1 < u_2 < u_3$, that are the equilibrium solutions of $F(u)$, this amounts solving the system of nonlinear equations:

$$F(u_1) = 0, \quad F(u_2) = 0, \quad F(u_3) = 0;$$

we do this by employing a quasi-Newton method (cf. [28]) using the coefficients from the periodic solution of the conduit equation as the initial guess, see (33), achieving the convergent results after 1 or 2 iterative steps, depending on the convergence tolerance. Once we get u , we may set z and $p = \left(1 - \frac{D}{c} \right) z'$ based on (36c) and (36d), respectively.

6 Numerical methods

As in [8, 10], we use a fractional-step approach for the numerical resolution of the hyperbolic conduit system: at each time step, we alternate between by solving the homogeneous (hyperbolic) part of the system (26)

$$\begin{bmatrix} 1/u + \lambda(z-u)/u \\ -z/c \\ p/c \end{bmatrix}_t + \begin{bmatrix} -\ln(u^2) \\ z \\ p \end{bmatrix}_x = 0 \quad (38a)$$

over a time step Δt , and the ODEs

$$\begin{bmatrix} 1/u + \lambda(z-u)/u \\ -z/c \\ p/c \end{bmatrix}_t = \begin{bmatrix} 0 \\ p \\ \lambda(z-u) \end{bmatrix} \quad (38b)$$

using the initial data from the previous step and the same time step. Here the numerical method we employed for (38a) is the same as for the conduit equation, see Appendix A. To update the solution of the ODEs (38b), we need to solve the linear second-order ODE:

$$z_{tt} + \frac{\lambda c^2 E_0}{E_0 + \lambda} z = \frac{\lambda c^2}{E_0 + \lambda} \quad (39a)$$

with the initial conditions

$$\left. \left(\frac{1}{u} + \lambda \frac{z-u}{u} \right) \right|_{t=0} = E_0, \quad z(0) = z_0, \quad p(0) = p_0. \quad (39b)$$

If $E_0 > 0$, its exact solution is:

$$z = \frac{1}{E_0} \left[1 + (E_0 z_0 - 1) \cos(\omega t) - \frac{c p_0 E_0}{\omega} \sin(\omega t) \right], \quad (40a)$$

where $\omega^2 = \lambda c^2 E_0 / (E_0 + \lambda)$. We then have

$$p = -\frac{1}{c} z_t = p_0 \cos(\omega t) + \frac{\omega (E_0 z_0 - 1)}{c E_0} \sin(\omega t). \quad (40b)$$

If $E_0 < 0$ ($E_0 + \lambda > 0$ for large λ), we find the exact solution:

$$z = \frac{1}{2E_0} \left[2 + \left(E_0 z_0 - 1 - \frac{c p_0 E_0}{\mu} \right) e^{\mu t} + \left(E_0 z_0 - 1 + \frac{c p_0 E_0}{\mu} \right) \exp^{-\mu t} \right], \quad (40c)$$

$$p = -\frac{1}{c} z_t = -\frac{\mu}{2cE_0} \left[\left(E_0 z_0 - 1 - \frac{c p_0 E_0}{\mu} \right) e^{\mu t} - \left(E_0 z_0 - 1 + \frac{c p_0 E_0}{\mu} \right) \exp^{-\mu t} \right], \quad (40d)$$

where $\mu^2 = -\lambda c^2 E_0 / (E_0 + \lambda)$. Recall that E_0 , z_0 and p_0 are the solution of the homogeneous system (38a).

7 Numerical results

For the tests below, we take a uniform mesh size $\Delta x = 0.05$, and a time step Δt determined from the Courant-Friedrich-Lewy (CFL) condition for the stability of the hyperbolic solver. The non-reflecting boundary condition was employed on the left and right of the boundaries during the computations. For comparison, we will present results obtained using four different schemes for the homogeneous system (38a): MUSCL, WENO3, WENO5, and BVD35, see Appendix A for the details. The ODEs (38b) is solved using the exact solution (40) in all cases.

Our first test is an example studied in [25] for solitary wave fission of a large disturbance in a viscous fluid conduit. In this test, the initial condition for the conduit equation is the box:

$$u(0, x) = 1 + \frac{1}{2}\alpha \left[\tanh\left(\frac{x-x_0}{\beta}\right) - \tanh\left(\frac{x-x_0-L}{\beta}\right) \right], \quad (41)$$

where $\alpha = 0.88$, $\beta = 2.5$, and $x_0 = 300$ for $x \in [0, 1500]$.

For the hyperbolic model, the parameter values we set for c and λ are 30 and 900, respectively.

Figure 3 shows numerical results for $L = 48$ and 96 at time $t = 350$ obtained using BVD35 case of the algorithm, observing good agreement of the state variable u between the conduit equation and its hyperbolic variant. In addition, we observe the similar solution structure between u and z which confirms the validity of our formal approach. For comparison, we repeat the computations using MUSCL, WENO3, and WENO5 cases. In Figure 4 we show snapshots of the state variable u at time $t = 350$ only partially in the region $x \in [1000, 1500]$ (for completeness, the BVD35 results are included). It is clear that among them WENO5 and BVD35 give better solutions than WENO3 and MUSCL. For the MUSCL case, in particular, it is surprising to see the nonconvergence on the phase and amplitude for the foregoing solitary waves; this may mean that the third-order truncation (dispersive) error is too large for this problem, when discretizing the hyperbolic conduit equation based on the MUSCL approach.

Our second test is an example studied in [10] for the BBM equation. In this test, for the conduit equation, we take the Gaussian profile:

$$u(0, x) = 1 + \frac{2}{\sqrt{\pi}} \exp(-x^2/L^2) \quad (42)$$

for $x \in [-200, 600]$. For the hyperbolic model, we use the same initialization procedure as before under (42), and the same parameter values for c and λ during the computations.

Figure 5 shows numerical results in the case of $L = 20$ and 50 at time $t = 150$ obtained using BVD35 case of the algorithm. We again observe good agreement of the state variable u between the conduit equation and its hyperbolic variant, and also the same solution behavior between u and z . As in the previous test, we perform the computations using MUSCL, WENO3, and WENO5 cases also,

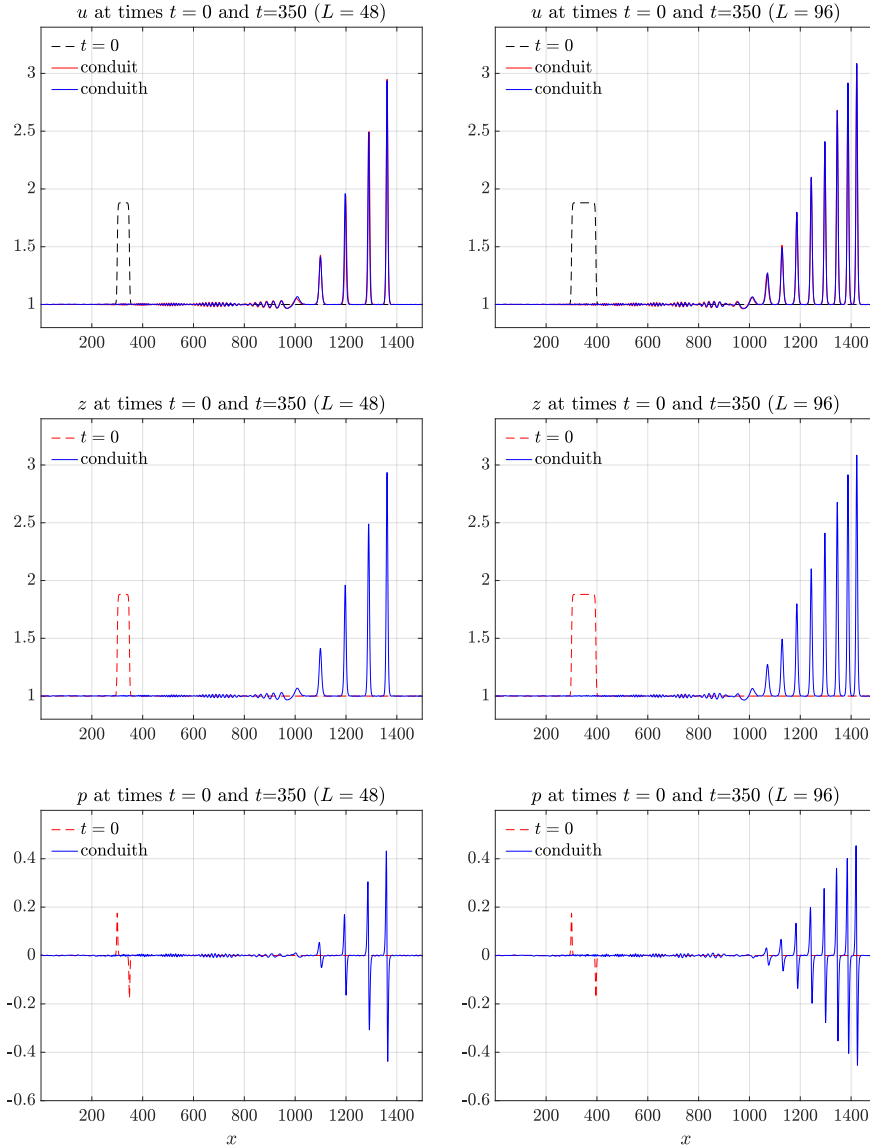


Figure 3: Numerical results for the first test. Snapshots of solutions obtained using BVD35 case of the method are shown at time $t = 350$ for $L = 48$ and $L = 96$. In both cases, parameter values $c = 30$ and $\lambda = 900$ were used in the computations. The blue line legend “conduith” means the results obtained using the hyperbolic approximation of the conduit equation, while the red line legend “conduit” is for the exact conduit equation.

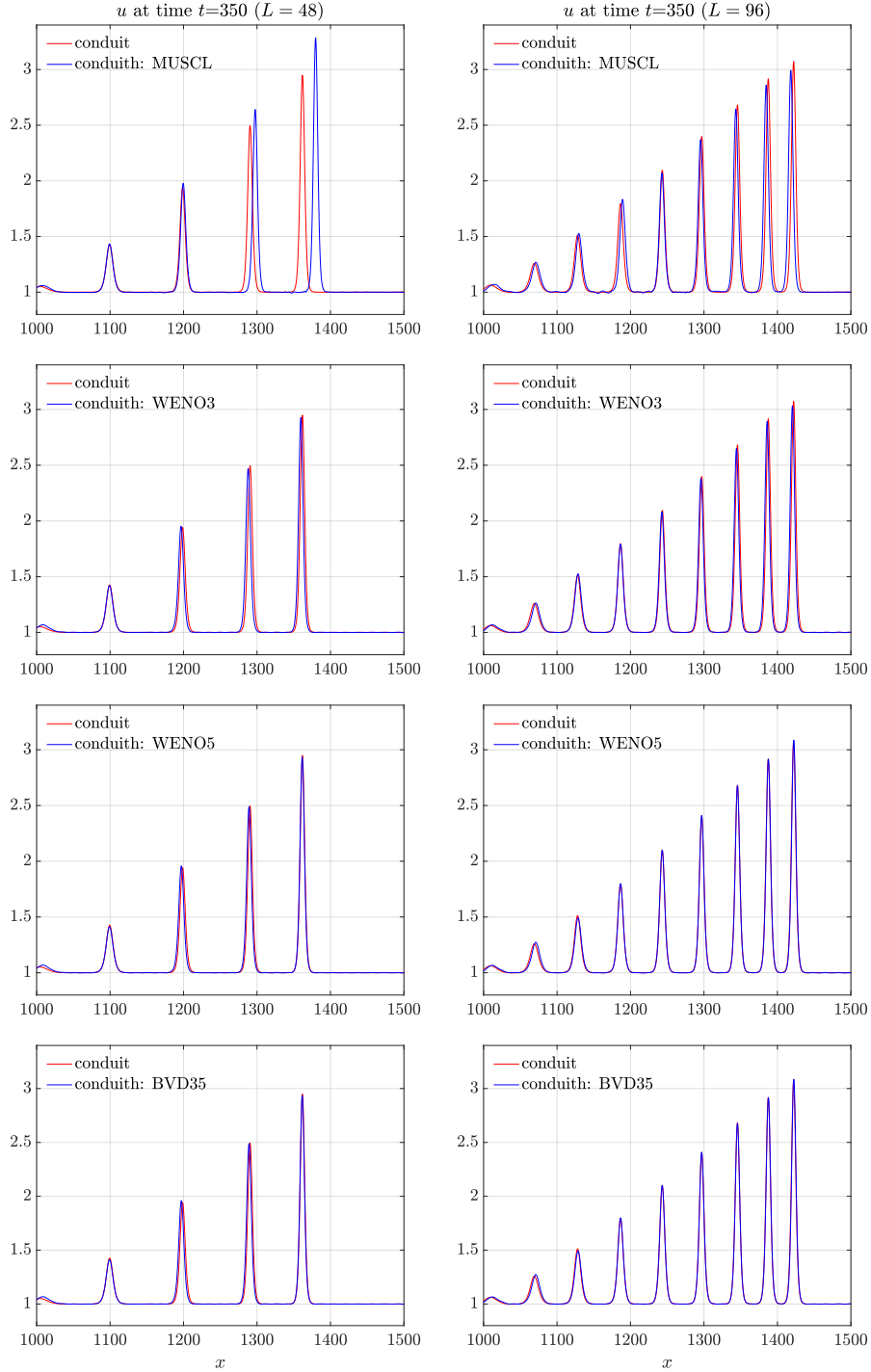


Figure 4: Numerical methods comparison for the first test. Snapshots of the state variable u obtained using four different hyperbolic solvers are shown at time $t = 350$ in the case of $L = 48$ and $L = 96$; only partial solutions in the region $x \in [1000, 1500]$ are shown. In both cases, parameter values $c = 30$ and $\lambda = 900$ were used in the computations.

Table 1: The CPU time (sec) taken for the numerical results shown in Fig. 7

	conduit	hyperbolic model	
		$c = 20$	$c = 100$
first test	1021.528	3057.535	14572.31
second test	247.996	1238.719	6150.387

and show numerical results in Figure 6; only the partial solutions in the region $x \in [200, 600]$ are shown. We find sensible good agreement of the solutions, even in the MUSCL case.

To show the convergence of the hyperbolic conduit solution to the conduit one, we perform a parameter study on c and $\lambda = c^2$ for $c = 20$ and 100. In Figure 7, the solutions of u for the first test in the case of $L = 96$ and the second test in the case of $L = 50$ are shown at times $t = 350$ (the first row) and $t = 150$ (the second row), respectively. Here, for clarity, only the partial solutions in the region $x \in [1210, 1450]$ and $x \in [300, 530]$ are drawn. It is clear that the solution is more accurate when a larger parameter is used in the computations. Table 1 gives the timing study in CPU (sec) for the results shown in Fig. 7, where the tests were performed in a Mac mini M2 Pro with 32GB RAM. We observe the higher computational cost when the hyperbolic model (26) is used as compared to the dispersive conduit equation (2).

8 Generalized Riemann problem

We call a generalized Riemann problem (GRP) the Cauchy problem

$$u(0, x) = \begin{cases} u_L(x), & x < 0, \\ u_R(x), & x > 0, \end{cases} \quad (43)$$

where u_L and $u_R(x)$ are different periodic travelling wave solutions of the corresponding dispersive equations (in particular, of the conduit equation). Such a problem was studied in [11] for the Serre-Green-Naghdi and Boussinesq equations with linear dispersion, in [10] for the BBM equation, and in [31] for the fifth order KdV equation. In particular, in the first reference new stable shock-like travelling wave solutions were found linking a constant solution (denoted further by u_*) to a periodic wave train. The shock-like transition zone between the constant state and the wave train was well described by the half of solitary wave having the wave crest at the maximum of the nearest periodic wave. Such a configuration was stable under certain conditions. For example, for the BBM equation such a shock-like structure is stable if the phase velocity of the periodic wave train is not less than the solution wave averaged representing indeed the characteristic velocity of a dispersionless homogeneous state [10]. In our case, the characteristic velocity of the dispersionless equation ($u_t + (u^2)_x = 0$) is $2u$. Since the dispersive properties of the BBM equation are similar to those of the

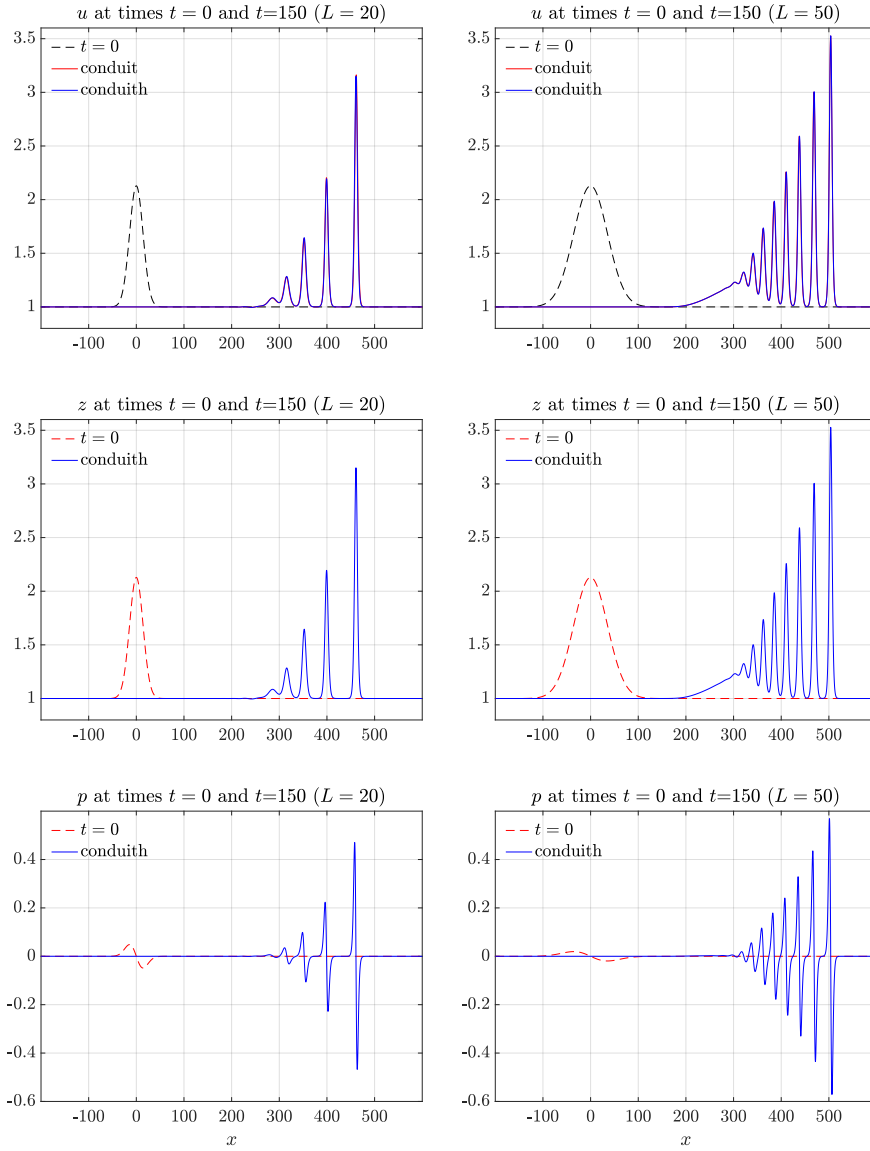


Figure 5: Numerical results for the second test. Snapshots of solution obtained using BVD35 case of the method are shown at time $t = 150$ for $L = 20$ and $L = 50$. In both cases, parameter values $c = 30$ and $\lambda = 900$ were used in the computations.

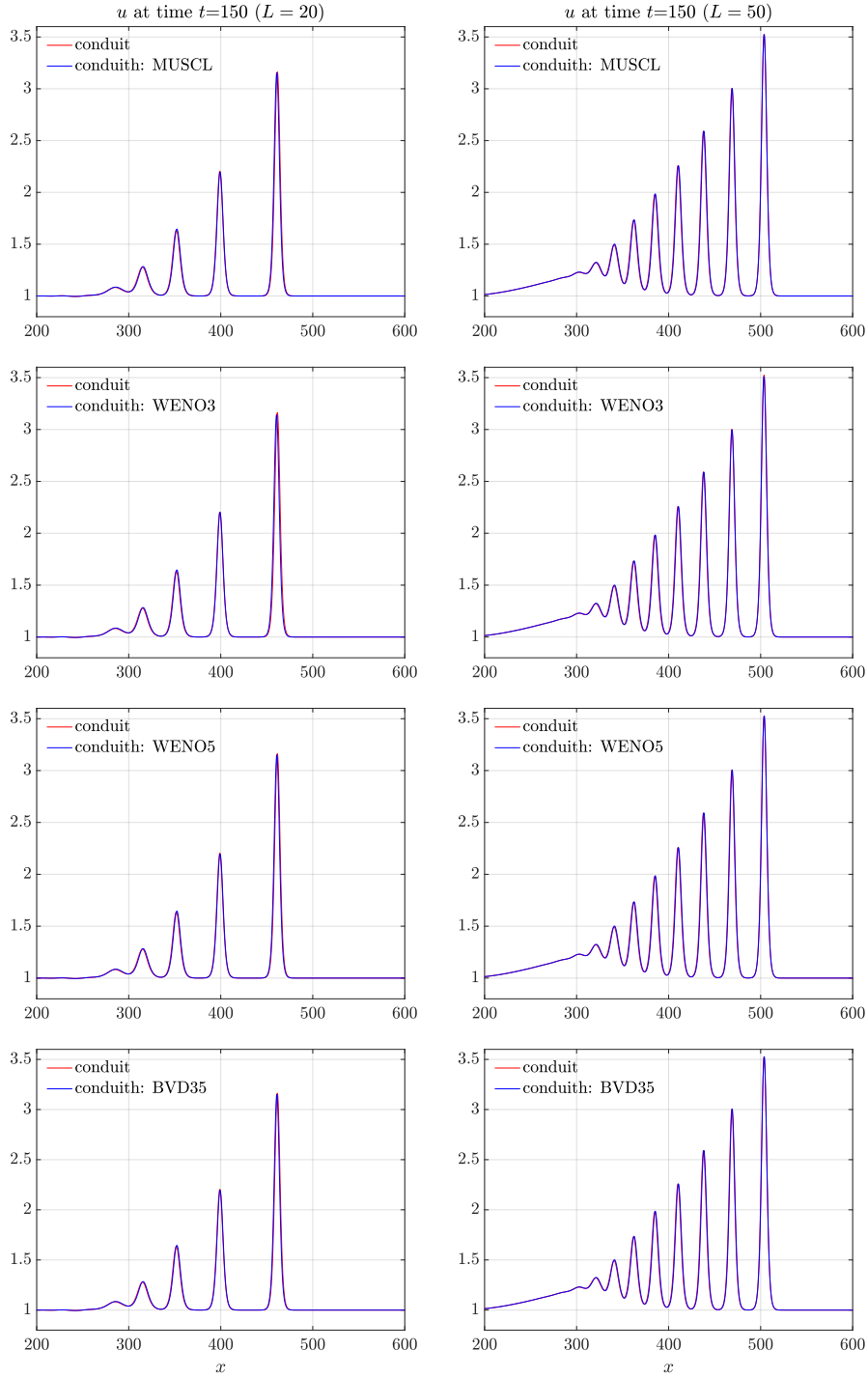


Figure 6: Numerical methods comparison for the second test. Snapshots of the state variable u obtained using four different hyperbolic solvers are shown at time $t = 150$ for $L = 20$ and $L = 50$; only the partial solutions in the region $x \in [200, 600]$ are shown. In both cases, parameter values $c = 30$ and $\lambda = 900$ were used in the computations. 16

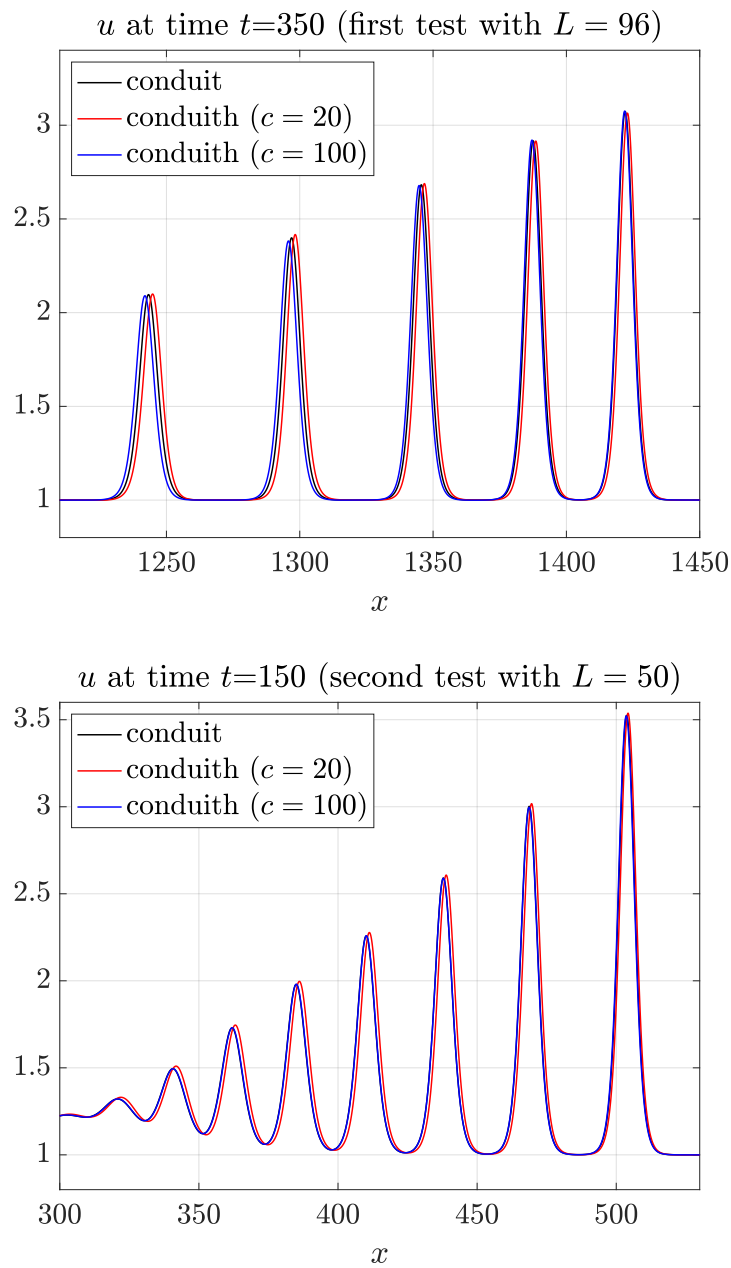


Figure 7: A parameter study of the solutions on c and $\lambda = c^2$ for the hyperbolic model. On the first row, the solutions are for the first test in the case of $L = 96$ at time $t = 350$, and on the second row, the solutions are for the second test in the case of $L = 50$ at time $t = 150$; only the snapshots of the state variable u are shown together with the conduit solution. In both cases, we used parameter values $c = 20$ and $c = 100$ in the computations.

conduit equation, we expect that the stable configuration linking a constant state u_* to a periodic wave train having the velocity D can be also realized for $D > 2\bar{u}$ (see the definition (35) of the wave averaged.) The aim of this section is thus to reveal the analogous solutions for the conduit equation numerically.

We begin by looking into a modified version of (43) in the form

$$u(0, x) = \begin{cases} \bar{u}, & x < x_0, \\ u(x), & x_0 < x < x_1, \\ \bar{u}, & x > x_1, \end{cases} \quad (44)$$

where $u(x)$ is a wave profile that consists of N periodic waves in the interval (x_0, x_1) , and \bar{u} is the average value of a single periodic wave over a wavelength. In the numerical experiments performed here, the parameters we take for the initial periodic solution are $u_1 = 1$, $u_3 = 2$ and $u_2 = 2 - m_0$, $m_0 = 0.999$. Then with Wolfram Mathematica, Version 12, one gets the phase speed $D \approx 2.546$, the average state $\bar{u} \approx 1.216$, and the wave length $L \approx 42.72$. The initial wave train is formed by introducing $N = 48$ of such a periodic solution into one.

In Figure 8, we show the pseudo-color plot of the solution in (x, t) -plane, observing clearly the formation of a constant state u_* on the left of the primary periodic wave train and on the right of the left rarefaction wave. This is as expected, because as in [10] we have the phase speed $D \approx 2.546$ larger than the characteristic speed $2\bar{u} \approx 2.432$, a necessary condition for the existence of the stable shock-like travelling structure. The snapshot of the solution for the problem at time $t = 600$ is shown in Figure 9, where the solution shown on the left is obtained using the conduit equation, and on the right is obtained using the hyperbolic model. We observe good agreement of the results qualitatively.

To determine analytically the state u_* , we use the Rankine-Hugoniot relation coming from the conservative form (1) (the mass conservation law). We consider the jump relation for (1) on the travelling wave solutions for a shock having the same velocity D as that of the travelling wave train, and linking the maximum amplitude u_3 of the wave train with the constant state u_* (see [11, 10] for details)

:

$$-D(u_3 - u_*) + (u_3^2 - u_*^2 + u_3 Du''|_{u=u_3}) = 0 \quad (45)$$

We have used the fact that in the u_3 state and extremal state “star” the derivative u' vanishes. The states u_2 (minimum value of u), u_3 (maximum value of u) and the velocity D are related through the first integral :

$$Cu_2^2 - 2u_2^2 \ln(u_2) - 2Du_2 = Cu_3^2 - 2u_3^2 \ln(u_3) - 2Du_3 \quad (46)$$

It allows us to find C :

$$C = \frac{2u_3^2 \ln(u_3) + 2Du_3 - 2u_2^2 \ln(u_2) - 2Du_2}{u_3^2 - u_2^2}. \quad (47)$$

Hence, one can estimate Du'' at the maximum u_3 from (32) :

$$Du''|_{u=u_3} = (C - 1)u_3 - 2u_3 \ln(u_3) - D. \quad (48)$$

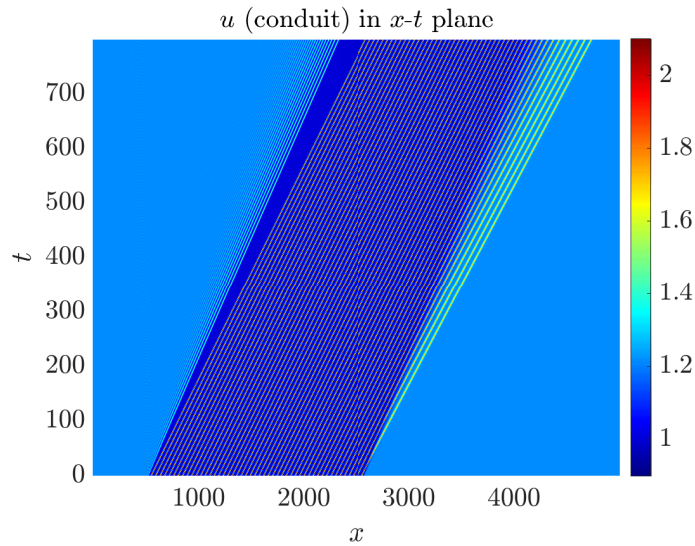


Figure 8: The general solution structure of Cauchy problem (44) for the conduit equation is shown in (x, t) -plane. The wave train in the middle consists of 48 periodic waves, where the initial parameters for each of them are: $u_1 = 1$, $u_3 = 2$ and $u_2 = 2 - m_0$, $m_0 = 0.999$. The wave average on the left and right of the wave train is $\bar{u} \approx 1.216$.

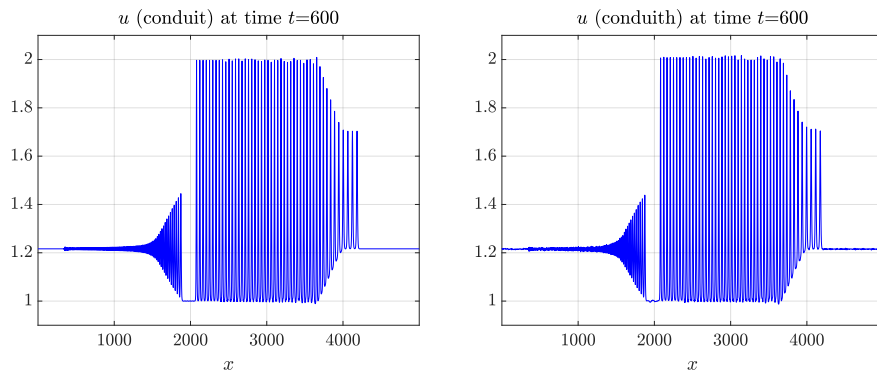


Figure 9: The snapshot of the solution for the Cauchy problem (44) at time $t = 600$. The solution shown on the left is obtained using the conduit equation, and on the right is obtained using the hyperbolic model with the parameters $c = 30$ and $\lambda = 900$.

We can now replace all into (45) to obtain the equation for u_* :

$$-D(u_3 - u_*) + (u_3^2 - u_*^2 + u_3(C u_3 - 2u_3 \ln(u_3) - u_3 - D)) = 0. \quad (49)$$

As for the BBM equation [10], one can prove that $u_1 < u_* < u_2$.

In particular, if we take the same u_2 , u_3 , and D as in the Cauchy problem (44), we find the value $u_* \approx 1.000499$. Then we may construct a multi-hump structure in the form

$$u(0, x) = \tilde{u}(x) = \begin{cases} u_*, & x < x_0, \\ u_M(x), & x_0 < x < x_1, \\ u_*, & x > x_1. \end{cases} \quad (50)$$

with u_M as a periodic wave train linked to u_* . Fig. 10, the left column, shows u_M composed of $N = 11$ periodic wave solutions. This multi-hump solution structure is a stable one as we can see in Fig. 11. Here we present the snapshot solutions obtained using the conduit equation and the hyperbolic model at time $t = 1000$.

We are next concerned with a double multi-hump problem for the interaction of two periodic wave trains. The initial condition is:

$$u(0, x) = \begin{cases} \tilde{u}_L(x), & x \leq x_0, \\ \tilde{u}_R(x), & x > x_0, \end{cases} \quad (51)$$

where \tilde{u}_L and \tilde{u}_R are having analogous structure to (50), see the right column of Fig. 10 for an illustration. To be specific, for each wave train it consists of $N = 11$ periodic waves together with a hybrid half wavelength periodic and solitary waves, and $x_0 = 1600$. The state values we take for \tilde{u}_L are $u_1^L = 0.9$, $u_2^L = 0.907$, $u_3^L = 1.7$, and that give $D_L \approx 2.25$, $\bar{u}_L \approx 1.123$, and $u_*^L \approx 0.903477$. For \tilde{u}_R , we have $u_1^R = 0.9$, $u_2^R = 0.907$, $u_3^R = 1.25$, and get $D_R \approx 2.01871$, $\bar{u}_R \approx 1.00894$, and $u_*^R \approx 0.903467$. Since the states u_*^L and u_*^R are approximately the same, and $D_L > D_R$, we can study the overtaking multi-hump soliton problem propagation on the same level u_* .

Figure 12 shows the numerical solutions for the conduit equation at times $t = 500, 2000, 2500, 3000, 4000, 5000$, observing the wave interaction, merging, and their full reconstruction. Here without introducing a large domain size, the computation domain is adjusted in time by the method to have the multi-hump solution stayed inside the region. The solutions for the hyperbolic model are shown in Fig. 13, we again observe good qualitative agreement of the solution, and the validation of the numerical solutions.

The stability of multi-hump solutions created “artificially” by combining periodic solutions and constant states related by the generalized Rankine-Hugoniot relations show that they are stable weak solutions to the conduit equation. In particular, they are stable under a “perturbation” of the conduit equation by a hyperbolic system conserving its original Godunov type form.

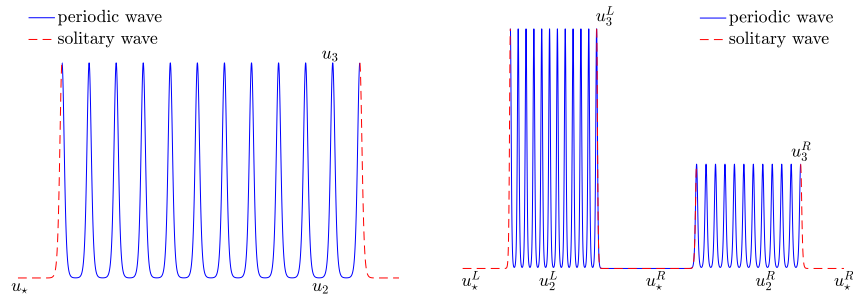


Figure 10: Illustration of the initial conditions for the multi-hump problems. The plot shown on the left is for the single hump problem (50), and on the right is for the double hump problem (51).

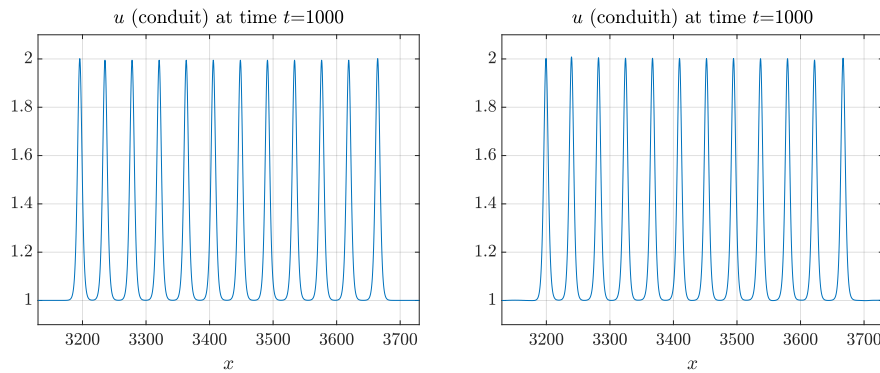


Figure 11: The snapshot of the conduit solution for the multi-hump problem (50) at time $t = 1000$. The solution on the left is for the conduit equation, and on the right is for the hyperbolic model. The computation domain is $x \in [0, 4000]$; only the partial solutions in the region $x \in [3130, 3730]$ are shown.

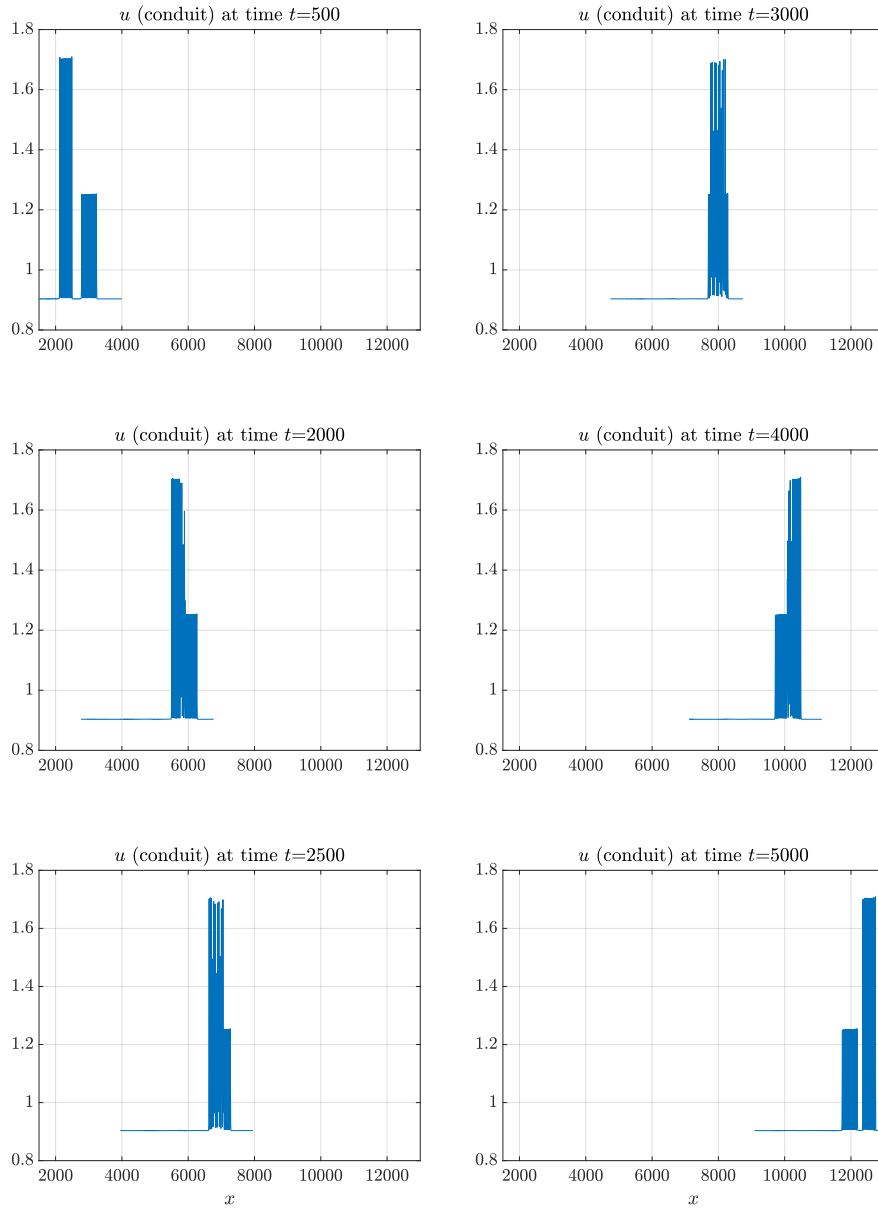


Figure 12: The snapshot of the conduit solution for the two multi-hump problem (51) at times $t = 500, 2000, 2500, 3000, 4000, 5000$. The plots are displayed from the left top to bottom and continues from the right top to bottom. The computation domain is adjusted in time to have the multi-hump solution stayed in the domain; only the partial solutions in the neighborhood of the multi-hump solitons are shown.

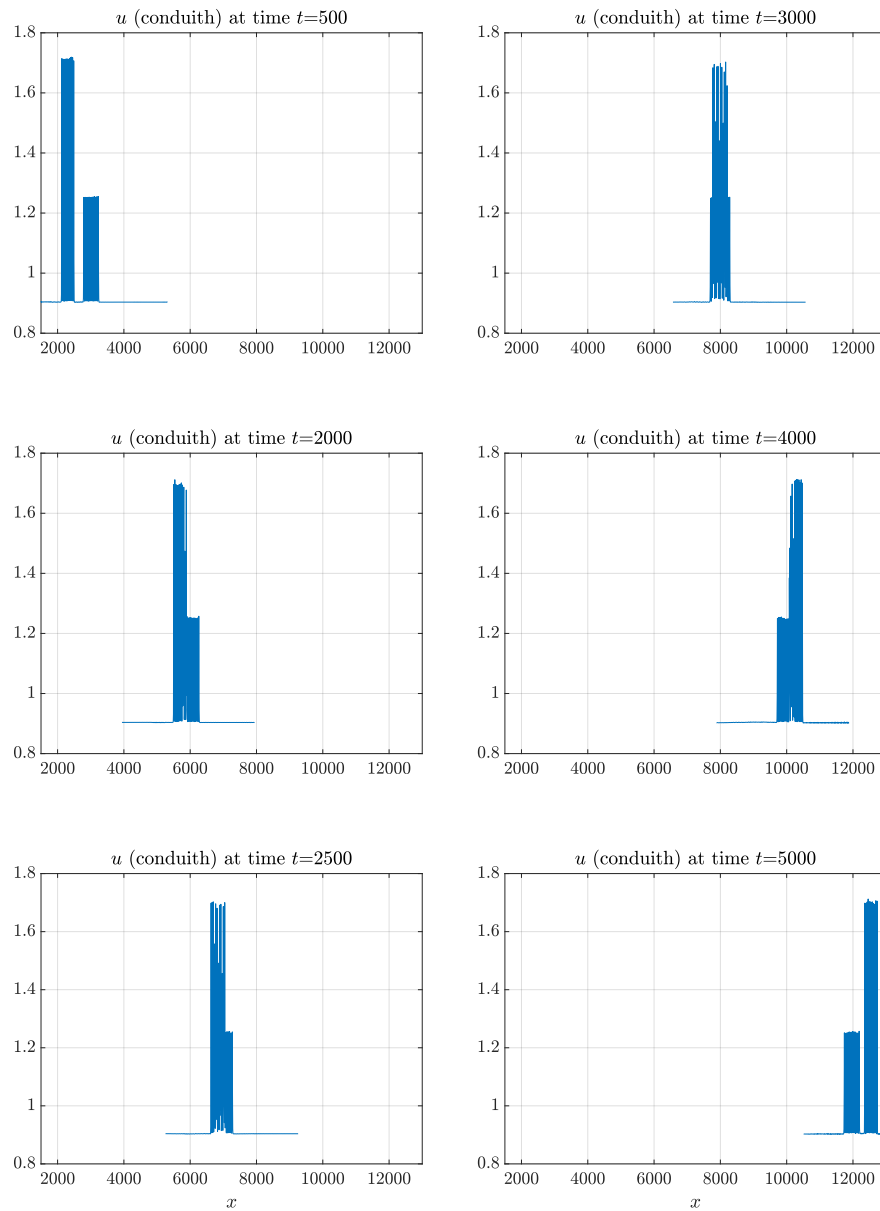


Figure 13: The snapshot solutions of the hyperbolic conduit model for the two multi-hump problem (51) at times $t = 500, 2000, 2500, 3000, 4000, 5000$. The plots are displayed in the same manner as Fig. 13.

9 Conclusion

We have proposed a hyperbolic approximation of the conduit equation preserving, in particular, invariance properties of the conduit equation (reversibility in time and space) and approximating the solutions of the conduit equation with good accuracy. The advantage of the hyperbolic approximation is that it allows all the numerical tools developed for hyperbolic equation systems to be applied to the study of dispersive equations.

We have constructed new solutions to the conduit equation representing an assemblage of many waves of the same period linked to a constant solution by the generalized Rankine-Hugonit relation, also taking into account the curvature of periodic waves. The generalized shock linking the maximum of the lateral periodic waves to a constant state has the same velocity as that of the periodic wave train. Such a multi-hump solitary wave is stable if the wave velocity is twice as great as \bar{u} . This condition means that the phase velocity of such a structure must be supercritical with respect to the homogeneous state \bar{u} having the characteristic slope $2\bar{u}$. The hyperbolic approximation of the conduit equation also admits such stable solutions.

Data Availability Statement

The computational codes developed for this research are available from the authors by request.

Declaration of competing interest

The authors have no conflicts of interest to declare that are relevant to the content of this article.

Ethics

The work is original, has not been published before, and is not currently being considered for publication elsewhere.

Acknowledgments SG was partially supported by Agence Nationale de la Recherche, France (SNIP ANR-19-ASTR-0016-01). KMS thanks the Institut Mécanique et Ingénierie of Marseille and INRIA - Sophia-Antipolis - Méditerranée for financial support during his stay at IUSTI, Marseille.

A Numerical methods for the conduit equation

To find approximate solutions to the conduit equation (2), we use the hyperbolic-elliptic splitting approach developed previously in [19, 11, 10]. This algorithm consists of two steps. In the first step, the hyperbolic step, we employ the state-of-the-art method for hyperbolic conservation laws for the numerical resolution of the equation

$$\mathcal{K}_t - (\ln u^2)_x = 0 \tag{52a}$$

over a time step Δt . In the second step, the elliptic step, using the approximate solution \mathcal{K} computed during the hyperbolic step, we invert numerically the elliptic operator:

$$-u_{xx} + \mathcal{K}u = 1 \tag{52b}$$

for u with prescribed boundary conditions based on a finite-difference scheme [21].

It should be mentioned that from (1) one can also find numerical solutions to the conduit equation when we apply the algorithm to solve the following hyperbolic-elliptic system:

$$u_t + (u^2 + \varpi)_x = 0, \quad (53a)$$

$$-\left(\frac{\varpi_x}{u}\right)_x + \frac{\varpi}{u^2} = 2u_{xx}, \quad (53b)$$

separately for u and ϖ during each time step.

More precisely, in the hyperbolic step, we use the semi-discrete finite volume method written in a wave-propagation form as before [11], but employ a different solution reconstruction technique, the BVD (boundary variation diminishing) principle, which is more robust than the classical one for the interpolated states (\mathcal{K} for (52) or u for (53)) at cell boundaries (cf. [5] and the references cited therein). These reconstructed variables form the basis for the initial data of the Riemann problems, where the solutions of the Riemann problems are then used to construct the fluctuations in the spatial discretization that gives the right-hand side of the system of ODEs (cf. [20, 17, 18]). To integrate the ODE system in time, the strong stability-preserving (SSP) multistage Runge-Kutta scheme [15, 30] is used. In particular, for the numerical results presented in this paper, the third-order SSP scheme was employed together with the pair of third- and fifth-order WENO (weighted essentially non-oscillatory) scheme in the BVD reconstruction process.

References

- [1] T. B. Benjamin, J. L. Bona, and J. J. Mahony. Model equations for long waves in nonlinear dispersive systems. *Philosophical Transactions of the Royal Society of London. Series A, Mathematical and Physical Sciences*, 272(1220):47–78, 1972.
- [2] C. Besse, S. Gavriluk, M. Kazakova, and P. Noble. Perfectly matched layers methods for mixed hyperbolic–dispersive equations. *Water Waves*, 4(3):313–343, 2022.
- [3] S. Bourgeois, N. Favrie, and B. Lombard. Dynamics of a regularized and bistable Ericksen bar using an extended Lagrangian approach. *International Journal of Solids and Structures*, 207:55–69, 2020.
- [4] S. Busto, M. Dumbser, C. Escalante, N. Favrie, and S. Gavriluk. On high order ADER discontinuous Galerkin schemes for first order hyperbolic reformulations of nonlinear dispersive systems. *Journal of Scientific Computing*, 87(2):48, 2021.
- [5] X. Deng, S. Inaba, B. Xie, K. M. Shyue, and F. Xiao. High fidelity discontinuity-resolving reconstruction for compressible multiphase flows with moving interfaces. *J. Comput. Phys.*, 371:945–966, 2017.

- [6] F. Dhaouadi, N. Favrie, and S. Gavriluk. Extended Lagrangian approach for the defocusing nonlinear Schrödinger equation. *Studies in Applied Mathematics*, 142(3):336–358, 2019.
- [7] V. Duchêne. Rigorous justification of the Favrie–Gavriluk approximation to the Serre–Green–Naghdi model. *Nonlinearity*, 32:3772–3797, 2019.
- [8] N. Favrie and S. Gavriluk. A rapid numerical method for solving Serre–Green–Naghdi equations describing long free surface gravity waves. *Nonlinearity*, 30(7):2718, 2017.
- [9] S. Gavriluk and K.M. Shyue. Singular solutions of the BBM equation: analytical and numerical study. *Nonlinearity*, 35(1):388, 2021.
- [10] S. Gavriluk and K.M. Shyue. Hyperbolic approximation of the BBM equation. *Nonlinearity*, 35(3):1447, 2022.
- [11] S.L. Gavriluk, B. Nkonga, K.M. Shyue, and L. Truskinovsky. Stationary shock-like transition fronts in dispersive systems. *Nonlinearity*, 33:5477–5509, 2020.
- [12] S.L. Gavriluk and S.M. Shugrin. Media with equations of state that depend on derivatives. *Journal of Applied Mechanics and Technical Physics*, 37:177–189, 1996.
- [13] S.K. Godunov. An interesting class of quasi-linear systems. *Dokl. Akad. Nauk SSSR*, 139(3):521–523, 1961.
- [14] S.K. Godunov and E. Romenskii. *Elements of Continuum Mechanics and Conservation Laws*. Springer US, 2003.
- [15] S. Gottlieb, C. W. Shu, and E. Tadmor. Strong stability–preserving high–order time discretization methods. *SIAM Review*, 43:89–112, 2001.
- [16] M. A. Johnson and W.R. Perkins. Modulational instability of viscous fluid conduit periodic waves. *SIAM Journal of Mathematical Analysis*, 52(1), 2020.
- [17] D. I. Ketcheson and R. LeVeque. WenoClaw: A higher order wave propagation method, in: *Hyperbolic problems: Theory, numerics, applications*. *IMA journal of applied mathematics*, pages 609–616, 2005.
- [18] D. I. Ketcheson, M. Parsani, and R. LeVeque. High-order wave propagation algorithm for hyperbolic systems. *SIAM J. Sci. Comput.*, 35(1):A351–A377, 2013.
- [19] O. Le Métayer, S. Gavriluk, and S. Hank. A numerical scheme for the Green–Naghdi model. *J. Comp. Phys.*, 229:2034–2045, 2010.
- [20] R. J. LeVeque. *Finite Volume Methods for Hyperbolic Problems*. Cambridge University Press, 2002.

- [21] R.J. LeVeque. *Finite Difference Methods for Ordinary and Partial Differential Equations: Steady-State and Time-Dependent Problems*. SIAM, Philadelphia, 2007.
- [22] N.K. Lowman and M.A. Hoefer. Dispersive hydrodynamics in viscous fluid conduits. *Phys. Rev. E*, 88:023016, 2013.
- [23] N.K. Lowman and M.A. Hoefer. Dispersive shock waves in viscously deformable media. *J. Fluid. Mech.*, 718:524–557, 2013.
- [24] N.K. Lowman, M.A. Hoefer, and G.A. El. Interactions of large amplitude solitary waves in viscous fluid conduits. *J. Fluid. Mech.*, 750:372–384, 2014.
- [25] M.D. Maiden, N.A. Franco, E.G. Webb, G.A. El, and M.A. Hoefer. Solitary wave fission of a large disturbance in a viscous fluid conduit. *J. Fluid Mech.*, 883:A10, 2020.
- [26] M.D. Maiden and M.A. Hoefer. Modulations of viscous fluid conduit periodic waves. *Proc. R. Soc. A*, 472:20160533, 2016.
- [27] M.D. Maiden, N.K. Lowman, D.V. Anderson, M.E. Schubert, and M.A. Hoefer. Observation of dispersive shock waves, solitons, and their interactions in viscous fluid conduits. *Phys. Rev. Lett.*, 116:174501, 2016.
- [28] J. Nocedal and S.J. Wright. *Numerical Optimization*. Springer, second edition, 2006.
- [29] P. Olson and U. Christensen. Solitary wave propagation in a fluid conduit within a viscous matrix. *J. Geo. Research*, 91:6367–6374, 1986.
- [30] C. W. Shu. High order weighted essentially nonoscillatory schemes for convection dominated problems. *SIAM Review*, 5:82–126, 2009.
- [31] P. Sprenger and M. A. Hoefer. Discontinuous shock solutions of the Whitham modulation equations as dispersionless limits of travelling waves. *Nonlinearity*, 33:3268–3302, 2020.
- [32] S. Tkachenko, S. Gavriluk, and J. Massoni. Extended Lagrangian approach for the numerical study of multi-dimensional dispersive waves: applications to the Serre–Green–Naghdi equations. *Journal of Computational Physics*, 477:111901, 2023.